

## MIT Open Access Articles

*Chemical Characterization of the Smallest S-Nitrosothiol, HSNO; Cellular Cross-talk of H<sub>2</sub>S and S-Nitrosothiols*

The MIT Faculty has made this article openly available. **Please share** how this access benefits you. Your story matters.

**Citation:** Filipovic, Milos R., Jan Lj. Miljkovic, Thomas Nauser, et al. 2012. Chemical Characterization of the Smallest S -Nitrosothiol, HSNO; Cellular Cross-talk of H<sub>2</sub>S and S - Nitrosothiols. *Journal of the American Chemical Society* 134(29): 12016–12027.

**As Published:** <http://dx.doi.org/10.1021/ja3009693>

**Publisher:** American Chemical Society

**Persistent URL:** <http://hdl.handle.net/1721.1/79076>

**Version:** Final published version: final published article, as it appeared in a journal, conference proceedings, or other formally published context

**Terms of Use:** Article is made available in accordance with the publisher's policy and may be subject to US copyright law. Please refer to the publisher's site for terms of use.



# Chemical Characterization of the Smallest S-Nitrosothiol, HSNO; Cellular Cross-talk of H<sub>2</sub>S and S-Nitrosothiols

Milos R. Filipovic,<sup>\*,†</sup> Jan Lj. Miljkovic,<sup>†</sup> Thomas Nauser,<sup>‡</sup> Maksim Royzen,<sup>§</sup> Katharina Klos,<sup>†</sup> Tatyana Shubina,<sup>||</sup> Willem H. Koppenol,<sup>‡</sup> Stephen J. Lippard,<sup>§</sup> and Ivana Ivanović-Burmazović<sup>†</sup>

<sup>†</sup>Department of Chemistry and Pharmacy, University of Erlangen-Nürnberg, 91058 Erlangen, Germany

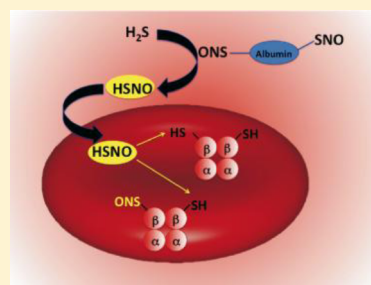
<sup>‡</sup>Institute of Inorganic Chemistry, Department of Chemistry and Applied Biosciences, ETH Zürich, 8093 Zürich, Switzerland

<sup>§</sup>Department of Chemistry, Massachusetts Institute of Technology, 77 Massachusetts Avenue, Cambridge, Massachusetts 02139, United States

<sup>||</sup>Computer Chemistry Center, University of Erlangen-Nürnberg, 91052 Erlangen, Germany

## S Supporting Information

**ABSTRACT:** Dihydrogen sulfide recently emerged as a biological signaling molecule with important physiological roles and significant pharmacological potential. Chemically plausible explanations for its mechanisms of action have remained elusive, however. Here, we report that H<sub>2</sub>S reacts with S-nitrosothiols to form thionitrous acid (HSNO), the smallest S-nitrosothiol. These results demonstrate that, at the cellular level, HSNO can be metabolized to afford NO<sup>+</sup>, NO, and NO<sup>-</sup> species, all of which have distinct physiological consequences of their own. We further show that HSNO can freely diffuse through membranes, facilitating transnitrosation of proteins such as hemoglobin. The data presented in this study explain some of the physiological effects ascribed to H<sub>2</sub>S, but, more broadly, introduce a new signaling molecule, HSNO, and suggest that it may play a key role in cellular redox regulation.



## INTRODUCTION

Nitrogen monoxide and dihydrogen sulfide are two gaseous transmitters that regulate numerous physiological functions. Although the chemistry,<sup>1a–d</sup> biochemistry,<sup>1d,e</sup> and physiology<sup>1f,g</sup> of NO<sup>•</sup> have been widely studied since its identification as the endothelium-derived relaxing factor,<sup>1h</sup> H<sub>2</sub>S has only recently been recognized as an important signaling molecule with physiological effects similar to those of nitrogen monoxide.<sup>2</sup> A (bio)chemical understanding of its mechanism of action is minimal, however.<sup>3</sup> Although some authors have proposed interplay between NO<sup>•</sup> and H<sub>2</sub>S signaling pathways,<sup>4</sup> it is widely accepted that the physiological consequences of H<sub>2</sub>S, unlike NO, do not directly involve cyclic guanosine monophosphate (cGMP).<sup>5</sup>

One of the modes of NO<sup>•</sup> signaling is activation of soluble guanylate cyclase to produce cGMP.<sup>1f</sup> Another, equally important role of NO<sup>•</sup> action is S-nitrosation.<sup>6a</sup> Two decades after characterization of the first S-nitrosothiols in biological systems,<sup>1e</sup> S-nitrosation of ~1000 proteins has been reported, and this posttranslational modification is increasingly considered to be as important as phosphorylation.<sup>6</sup> The mechanism of S-nitrosation and signaling through formal transfer of the “NO<sup>+</sup>” moiety is still a matter of debate, however.<sup>6c</sup> It has been recently proposed<sup>4e</sup> that H<sub>2</sub>S may play a role in modulating the S-nitrosothiol profile in the cells, and we hypothesized that this mechanism may involve the reaction of hydrogen sulfide with low-molecular weight and/or protein S-nitrosothiols (RSNOs) to form the smallest S-nitrosothiol, thionitrous acid (HSNO).<sup>7</sup>

Although extensively examined by computational methods,<sup>8,9</sup> HSNO has never been proved to exist in aqueous solution or characterized under physiologically relevant conditions. It has only been isolated and spectroscopically identified in an argon matrix at 12 K.<sup>10</sup> In the reaction of elementary sulfur and bis(triphenylphosphine)iminium nitrite, (PNP<sup>+</sup>)(NO<sub>2</sub><sup>-</sup>), upon addition of triphenylphosphine under vacuum in pure organic water free solvents, (PNP<sup>+</sup>)(SNO<sup>-</sup>) has been characterized.<sup>11</sup>

Here, we prove the existence of HSNO under physiologically relevant conditions and demonstrate in vitro and at the cellular level that HSNO can serve as a source of NO<sup>+</sup>, NO<sup>•</sup>, and NO<sup>-</sup> entities, all of which evoke their own distinctive physiological responses. Furthermore, we show that HSNO can freely diffuse through membranes facilitating transnitrosation of proteins.

## EXPERIMENTAL SECTION

**Materials.** All chemicals were of the highest purity available and purchased from Sigma-Aldrich. Buffers were prepared with nanopure water and further purified and stored over Chelex-100 to remove traces of transition metals. All experiments were performed using anhydrous Na<sub>2</sub>S (Sigma Aldrich),<sup>12</sup> which was stored in a glovebox under argon (<1 ppm O<sub>2</sub> and <1 ppm H<sub>2</sub>O). Stock solutions (100 mM) of sodium sulfide were prepared in the glovebox using argon-saturated nanopure water and stored in glass vials with PTFE septa at 4 °C for no longer than 1 week. Gas-tight Hamilton syringes were used to transfer these solutions throughout our studies.<sup>13</sup>

Received: January 30, 2012

Published: June 28, 2012

**Analysis of NO<sup>•</sup> and H<sub>2</sub>S.** The fate of hydrogen sulfide and nitrogen monoxide during the course of the reaction was monitored with a 2 mm shielded H<sub>2</sub>S sensor and the ISO-NO probe (World Precision Instruments), connected to a Free Radical Analyzer (World Precision Instruments).<sup>13</sup> Electrode responses were monitored using DataTrax software for signal processing. Experiments were performed in a four-channel chamber (WPI) with both electrodes running either simultaneously or individually. A 2 mL portion of 50 mM pH 7.4 potassium phosphate (KPi) buffer was added to the reaction chamber before immersion of the electrodes. Depending on the type of measurement, different concentrations of sodium sulfide (50–500  $\mu$ M) were injected followed by addition of S-nitrosoalbumin (GSNO) or S-nitrosoalbumin.

**UV/Vis Spectrometric Studies.** All spectrophotometric studies were performed on a Hewlett-Packard 8452A diode array spectrophotometer connected to a Dell computer operating with Olis SpectralWorks software.

**GC–MS Detection of N<sub>2</sub>O.** A 5 mM GS<sup>15</sup>NO solution in 50 mM pH 7.4 potassium phosphate buffer was degassed with argon and kept in dark glass vials sealed with PTFE septa. Sodium sulfide was added to yield a final concentration of 5 or 17.5 mM. GC–MS analyses were performed on a Bruker GC 450 TQ MS 300 instrument. The gas chromatograph was equipped with a capillary column Varian, VF-5 m. A 50  $\mu$ L volume of headspace gas was injected (splitless mode), and the following oven temperature program was used with helium as carrier gas: 5 min at 50 °C, then increased to 155 °C at a rate of 10 °C/min, and then increased to 260 °C at a rate of 30 °C/min. The positive electron impact ionization mode was used. Detector multiplier voltage was set to 1400 V, and the detection was performed by selected ion monitoring of  $m/z$  46 (<sup>15</sup>N<sub>2</sub>O) and  $m/z$  31 (<sup>15</sup>NO) using a dwell time of 50 ms and scan width for SIM of 0.7 au. Areas under the peaks were determined using software provided by the manufacturer.

**GC–MS Detection of Hydroxylamine.** A 100  $\mu$ L sample of a hydroxylamine standard solution in 50 mM phosphate buffer at pH 7.4 was treated with 200  $\mu$ L of cyclopentanone, 2  $\mu$ L of concentrated sulphuric acid, and 1 mL of HPLC–MS grade methanol. After 1 h of incubation, the samples were diluted 10 times in methanol and injected into the GC–MS. The gas chromatograph was equipped with a Varian, VF-5 m capillary column. A 5  $\mu$ L volume of solution was injected (splitless mode) and the sample eluted using a 15 °C/min ramp from 50 to 250 °C. The positive electron impact ionization mode was used. The detector multiplier voltage was set to 1400 V, and the detection was performed by selected ion monitoring of  $m/z$  84 (cyclopentanone) and  $m/z$  99 (cyclopentanone oxime) using a dwell time of 50 ms and scan width for SIM of 0.3 au. Linear dependence of the area under the peak versus concentration of hydroxylamine was observed in the 2–100  $\mu$ M range.

**<sup>15</sup>N NMR Spectroscopic Characterization of HSNO.** Spectra of <sup>15</sup>N-labeled S-nitrosoalbumin (GS<sup>15</sup>NO, 25 mM), either with or without addition of sodium sulfide (25 mM), in 300 mM potassium phosphate buffer (pH 7.4) were recorded using a Bruker 400 MHz spectrometer (reference <sup>15</sup>N-nitromethane, at 50.67 MHz, 35° pulse width, 5 s relaxation delay).<sup>14</sup>

**FTIR Spectroscopy for in Situ Characterization of HSNO.** GSNO or GS<sup>15</sup>NO (120 mM) in 300 mM potassium phosphate buffer, pH 7.4, was monitored in solution (ReactIR 45 m, Mettler Toledo) utilizing a DiComp AgX fiber probe with diamond ATR element and MCT detector for 25 min to confirm stability prior to addition of Na<sub>2</sub>S (100 mM). Thereafter, spectra were recorded for 10 min, with each spectrum representing an average of 256 scans collected over 1 min in the range 900–1900 cm<sup>−1</sup>. A difference spectrum was obtained by subtracting the initial GSNO spectrum from all subsequent spectra.

**Pulse Radiolysis.** Generation of HS<sup>•</sup> and NO<sup>•</sup> by pulse radiolysis was performed as previously described.<sup>15</sup> Briefly, these free radicals were generated by irradiation of 1.2 mM Na<sub>2</sub>S and 0.12 mM KNO<sub>2</sub> in Ar-saturated water pH = 11 with electron pulses of 2 MeV energy and 20–50 ns duration generated by a Febetron 705 accelerator (Titan, San Leandro, CA).<sup>16</sup> A 300  $\mu$ L capacity quartz cell was used, and a

flow system ensured that each sample was exposed only to a single electron pulse.

**Cell Culture and HNO Bioimaging Studies.** Human umbilical vein endothelial cells (HUVECs, passage 2–3) were obtained from PromoCell GmbH (Heidelberg, Germany) and cultured in 35 mm  $\mu$ -Dishes (ibidi, Martinsried, Germany) in endothelial cell growth medium 2 (PromoCell GmbH) at 37 °C and 5% CO<sub>2</sub>. For HNO detection, HUVECs were incubated with 10  $\mu$ M of a nitroxyl-responsive dye (CuBOT1)<sup>17</sup> for 20 min. Cells were washed of excess fluorescent dye three times, placed into new medium, and further treated as specified in the figure legends. Fluorescence microscopy was carried out using an inverted microscope (Axiovert 40 CLF, Carl Zeiss), equipped with green fluorescent filters and ICM1 AxioCam. Images were postprocessed using ImageJ software, NIH, for semiquantitative determination of fluorescence intensity.

**S-Nitrosothiol Immunocytochemistry.** HUVECs were exposed to medium supplemented with 1 mM L-NAME, 1 mM propargylglycine, or both for 2 h and then fixed with 4% formaldehyde. Cells were permeabilized, blocked, and incubated with primary monoclonal, mouse anti-S-nitrosocysteine antibodies (Abcam, Cambridge, UK) following the instructions of the manufacturer. FITC-labeled, goat antimouse Fc-IgG antibodies (Sigma Aldrich, St. Louis, MO) were used as secondary antibodies.

**Transnitrosation of Albumin.** GSNO (1 mM) was incubated with (1 mM) sodium sulfide in 300 mM KPi, pH 7.4, for 3 min. Spectrophotometric measurements confirmed that all GSNO had reacted within 1 min. A 200  $\mu$ M portion of bovine serum albumin (BSA) was added to the solution and incubated for 15 min, dialyzed against water for 24 h, and prepared for MS analysis in acetonitrile/methanol (1:1, v/v) containing 0.1% formic acid.

**Protein-to-Protein Trans-nitrosation Mediated by HSNO.** To test the possibility that HSNO can serve as a small, easily diffusible trans-nitrosating agent, a special experimental setup was devised. Poly-S-nitrosoalbumin (BSA-SNO) was prepared by mixing 300  $\mu$ M BSA with 1 mM GSNO in the dark and incubation for 15 min, followed by 4 h dialysis against Chelex-resin 100-containing 50 mM KPi, pH 7.4, with constant exchange, and divided into two dialysis bags (cut off 5 kDa). A 1.5 mL portion of this material, serving as a control, was placed into a 15 mL Falcon tube containing 30  $\mu$ M BSA and incubated there for 5 min. To prove HSNO formation and that diffusion through the membrane takes place, 500  $\mu$ M Na<sub>2</sub>S was added into the other 1.5 mL of 300  $\mu$ M BSA-SNO, and the solution was dialyzed against 30  $\mu$ M BSA for 5 min. The entire experimental procedure was performed in the dark. Subsequently, the dialysis bag was removed and the external solution was analyzed for RSNO content using NO<sup>•</sup> and H<sub>2</sub>S electrodes,<sup>18</sup> Saville's method,<sup>19</sup> and the biotin-switch assay.<sup>20</sup>

**Transnitrosation of Hemoglobin in Red Blood Cells.** Red blood cells (RBCs) were obtained fresh from venous blood of healthy volunteers by centrifugation at 5000g for 5 min and washed three times with sterile PBS (Sigma Aldrich). RBCs were then resuspended in buffer to a cell count comparable to that of blood and used immediately. S-Nitrosoalbumin was prepared by mixing 300  $\mu$ M BSA with 1 mM CysNO in the dark and incubated for 15 min, followed by 4 h dialysis against Chelex resin-100-containing 50 mM KPi, pH 7.4, with constant exchange. A 30  $\mu$ M portion of this polynitroso-albumin was injected into 1 mL of RBC suspension, with or without further addition of 50  $\mu$ M Na<sub>2</sub>S or glutathione. After 5 min of incubation at room temperature, RBCs were centrifuged at 10 000g for 1 min, and the supernatant was replaced with fresh PBS. This procedure was repeated five times to ensure complete removal of residual RSNOs. RBC hemolysis was performed by addition of 3 volumes of nanopure water containing 100  $\mu$ M neocuproine, and obtained hemoglobin was further purified on Sephadex G-10 columns protected from light. All samples were adjusted to the same protein concentration and directly analyzed by Saville's assay<sup>19</sup> and/or ESI-TOF-MS.<sup>21</sup>

Additionally, 20  $\mu$ M washed RBC was diluted 100 $\times$  with PBS and exposed to 100  $\mu$ M poly BSA-SNO (prepared by acidification of BSA/nitrite mixture and then further purified on micro Bio Spin column) without or with addition of 100  $\mu$ M H<sub>2</sub>S, 100  $\mu$ M GSH, or 100  $\mu$ M Cys. Two minutes after the addition of BSA-SNO, the samples were

centrifuged for 3 min at 3000g and then washed with PBS three times prior to the hemolysis with nanopure water supplemented with 100  $\mu\text{M}$  neocuproine. Samples (20  $\mu\text{L}$ ) were separated on LC and subsequently analyzed by ESI-TOF-MS. LC separation was done using following protocol: column was equilibrated with a 50:50 mixture of buffer A (80:20, water:acetonitrile; 0.1% trifluoroacetic acid) and buffer B (40:60, water:acetonitrile; 0.1% trifluoroacetic acid) at a flow rate of 1 mL/min. Twenty microliters of each sample was loaded and eluted with a 2 min hold at 50% B, followed by a linear gradient to 66% B over 40 min.

**Mass Spectrometric Characterization.** All samples were analyzed using maXis (Bruker Daltonics), an ultrahigh-resolution ESI-TOF mass spectrometer operating in the positive ion mode. Data analysis, mass deconvolution, and spectra simulation were performed using data analysis software, provided by the manufacturer.

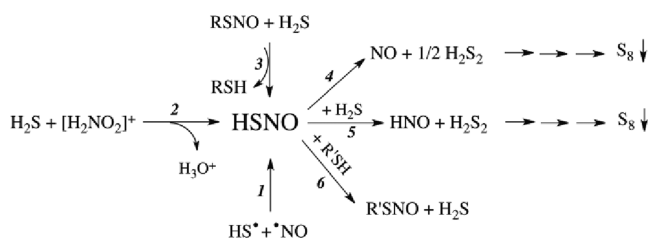
**Computational Methods.** Geometries of all structures were fully optimized at the B3LYP<sup>22a-d</sup> level of theory using the aug-cc-pVTZ<sup>22e-g</sup> basis set. Stationary points were confirmed to be minima or transition states by calculating the normal vibrations within the harmonic approximation. All computed relative energies are corrected for zero-point vibrational energies (ZPE). The Gaussian 09 program package was used for all of the above calculations.<sup>23</sup>

Thermochemical arguments are based on the group additivity approach described by Benson (see the Supporting Information) and standard electrode potentials.

## RESULTS AND DISCUSSION

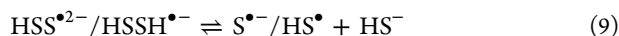
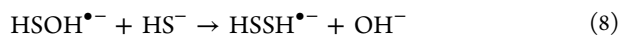
**Generation of HSNO/SNO<sup>-</sup> by Pulse Radiolysis.** To test whether HSNO could be generated in an aqueous solution, we performed pulse radiolysis experiments in which HS<sup>•</sup> and NO<sup>•</sup> (Scheme 1, eq 1) were cogenerated from HS<sup>-</sup>/nitrite-containing solutions (pH 11).

### Scheme 1. HSNO Generation (Eqs 1–3) and Reactivity (Eqs 4–6)



A broad peak around 370 nm is formed transiently after irradiation, reaching a maximum 5  $\mu\text{s}$  after irradiation (see Figure 1A). However, this spectrum comprises not only HSNO/SNO<sup>-</sup> but also precursors of HSNO/SNO<sup>-</sup> and side products formed during pulse radiolysis of nitrite and sulfide solutions.

HS<sup>-</sup> is oxidized to HS<sup>•</sup> via reactions given in eqs 7–9. Initially, HO<sup>•</sup> add to HS<sup>-</sup>, reaction 7,<sup>15</sup> with a rate constant  $k_1 = 5.4 \times 10^9 \text{ M}^{-1} \text{ s}^{-1}$  and, given the concentrations used, with a half-life of 110 ns. This oxidation step is followed by addition of hydrogen sulfide anion to yield disulfanuidyl, or dihydrogen disulfide radical anion (HSSH<sup>•-</sup>).



The reaction given in eq 8 has a half-life of 300 ns ( $k_2 \approx 2 \times 10^9 \text{ M}^{-1} \text{ s}^{-1}$ ).<sup>24a</sup> The HSSH<sup>•-</sup> product has an absorption maximum near 380 nm<sup>15</sup> (Figure 1A, red dots) and equilibrates

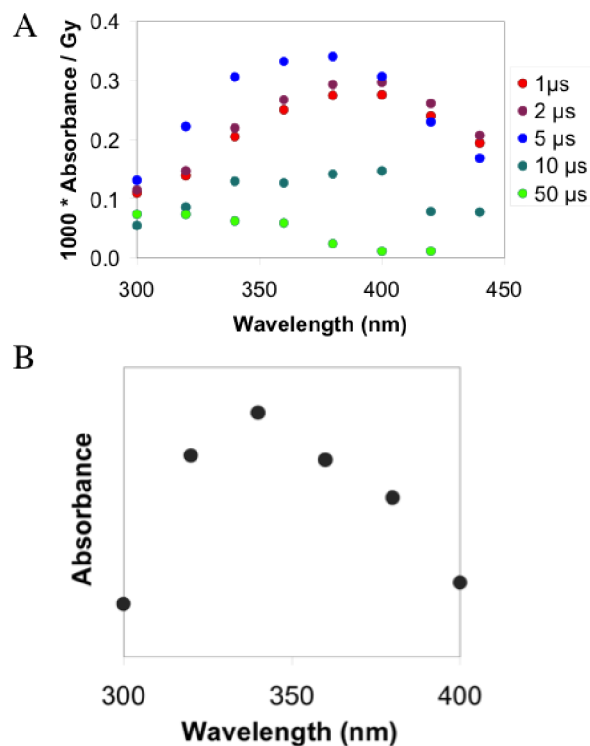
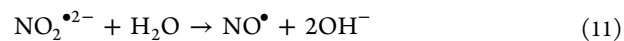


**Figure 1.** Generation of HSNO/SNO<sup>-</sup> by pulse radiolysis in argon-saturated water pH 11. (A) Time-resolved absorbance spectral investigation of HSNO/SNO<sup>-</sup> generated by pulse radiolysis. The spectra reveal formation of a peak at 370 nm consisting of HSSH<sup>•-</sup>/HSS<sup>• 2-</sup> and HSNO/SNO<sup>-</sup>. (B) The actual spectrum of generated HSNO/SNO<sup>-</sup>, obtained by subtracting the first spectrum from that acquired after 5  $\mu\text{s}$ .

very rapidly with HS<sup>•</sup>/S<sup>•-</sup> (eq 9), with a half-life of  $\sim 100 \text{ ns}$ <sup>24a</sup> ( $k_3 \approx 5 \times 10^5 \text{ s}^{-1}$ ,  $k_{-3} = 5.4 \times 10^9 \text{ M}^{-1} \text{ s}^{-1}$ ,  $K_3 \approx 10^{-4}$ ). With 1.2 mM HS<sup>-</sup> present, we expect 90% of the sulfur radicals to be present in the form of disulfanuidyl, which decays by mixed order.<sup>15</sup> Therefore, we have to assume that at least two different decay mechanisms compete with the desired reaction with NO<sup>•</sup>. Dominant at high radiation doses and, consequently, large radical concentrations is radical recombination leading to disulfide, which may trigger polysulfide production with an ill-defined reaction order.

Nitrogen monoxide is formed from NO<sub>2</sub><sup>-</sup> according to eqs 10 and 11:



The rate constant of reaction 10 is  $5 \times 10^9 \text{ M}^{-1} \text{ s}^{-1}$ , or, given the concentration of nitrite, that reaction has a half-life of approximately 1.2  $\mu\text{s}$ . Under first-order conditions, 90% conversion is reached after roughly 3 half-lives. Therefore, we observe initially (1  $\mu\text{s}$  after pulse) the spectrum of the disulfide radical anion with  $\lambda_{\text{max}} \approx 380 \text{ nm}$  (Figure 1A). Only after the production of NO<sub>2</sub><sup>• 2-</sup> or NO<sup>•</sup> does the desired radical recombination product, HSNO/SNO<sup>-</sup>, appear (Figure 1A). We assign the difference between the spectra before quantitative formation of NO<sup>•</sup> (1  $\mu\text{s}$  after pulse) and after its complete formation (5  $\mu\text{s}$  after pulse) to thionitrite, as nitrogen monoxide itself is colorless. As shown in Figure 1B, this spectrum has an absorbance maximum at 340 nm, a feature



characteristic of RSNOs that corresponds well to calculated values for  $\text{SNO}^-$ .<sup>24b</sup> Very rapid disappearance of the reaction product is expected because  $\text{HS}^-$  is in great excess under these experimental conditions and reacts with  $\text{HSNO/SNO}^-$  to generate  $\text{H}_2\text{S}_2$  and its deprotonated forms together with  $\text{HNO}$  (eq 5, Scheme 1). Furthermore, under the applied alkaline conditions,  $\text{HSNO/SNO}^-$  could hydrolyze according to reaction 12.



These processes all contribute to the short half-life of  $\text{HSNO/SNO}^-$  in the pulse radiolysis experiments. We therefore sought conditions for obtaining more stable  $\text{HSNO/SNO}^-$  preparations.

**HSNO/SNO<sup>-</sup> from the Reaction of Acidified Nitrite and H<sub>2</sub>S.** As shown in Scheme 1, eq 2, *S*-nitrosothiols could be generated from the acidified mixture of corresponding thiol and nitrite.<sup>19</sup> An attempt to synthesize  $\text{HSNO}$  by mixing sodium sulfide with acidified solution of sodium nitrite resulted in a transient color change, which was rapidly followed by decoloration and sulfur formation. Fast neutralization of the observed brownish reaction mixture gave a UV–vis spectrum with broad absorbance maximum at 370 nm, similar to that observed in pulse-radiolysis experiments (Figure S1A) consisting of dihydrogen disulfide radical anion, unreacted nitrite, and  $\text{HSNO/SNO}^-$ .

When analyzed by ESI-TOF-MS in the positive ion mode, the acidic reaction mixture showed a dominant peak at  $m/z$  64 (Figure S1B). Neutralization of the colored solution and subsequent MS analysis revealed the existence of the same peak at  $m/z$  63.9898 (100% abundance), which we ascribe to  $[\text{HSNO} + \text{H}]^+$  (Figure 2).

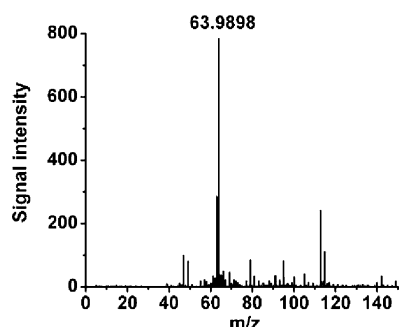


**Figure 2.** Mass spectrum of  $\text{HSNO}$ , that is,  $[\text{HSNO} + \text{H}]^+$ , prepared by acidification of nitrite in the presence of sulfide and then neutralized with the 300 mM potassium phosphate pH 7.4 buffer.

This might suggest that, at pH = 7.4, some  $\text{HSNO}$  present in solution. Recent experimental and computational work indicates that the  $\text{pK}_a$  value of an iron-coordinated  $\text{HSNO}$  intermediate is 10.5.<sup>25</sup> On the basis of that, free  $\text{HSNO}$  should have  $\text{pK}_a > 10.5$  and  $\text{HSNO}$  would be the major form under physiological conditions. However, comparing  $\text{HSNO}$  with  $\text{HNO}_2$ , one would expect a  $\text{pK}_a < 3.2$  and thus the anion as the predominant species at physiological pH. This issue remains to be resolved by future work.

**HSNO/SNO<sup>-</sup>, a Product of Transnitrosation between *S*-Nitrosoglutathione and H<sub>2</sub>S.** Although indicative of  $\text{HSNO}$  formation, the foregoing generation of the molecule under very acidic conditions is unlikely to be of physiological

relevance except perhaps for the stomach or acidic cell compartments. We therefore investigated the ability of  $\text{H}_2\text{S}$  to participate in transnitrosation reactions (Scheme 1, eq 3). Addition of equimolar amounts of  $\text{Na}_2\text{S}$  to buffered GSNO (*S*-nitrosoglutathione) solutions led to rapid (<1 min) formation of a yellow color (see Figure S2). A very similar UV–vis spectrum reported in the literature<sup>26</sup> was ascribed to  $\text{SSNO}^-$  as a product of this reaction.<sup>27</sup> However, the presence of other polysulfides in the reaction mixture can also be anticipated.

We analyzed the reaction mixture using ultrahigh-resolution ESI-TOF mass spectrometry. When mixed with  $\text{Na}_2\text{S}$ , the intensities of the main GSNO peaks decreased (see Figure S3) and new peaks appeared. The most intense is a peak at  $m/z$  345.0358, which we assign to  $[\text{GS}^\bullet + \text{K}]^+$  (or  $[\text{GSSG} + 2\text{K}]^{2+}$ ) (see Figure S3). More importantly, low-mass range spectral analysis revealed the formation of a new peak at  $m/z$  63.9902 (~5% of maximal intensity, similar to the spectrum observed in Figure 2).

Simulation of the isotopic distribution for  $[\text{HSNO} + \text{H}]^+$  and comparison of the calculated molecular weight (63.9852) with the obtained value unambiguously established its identity as  $\text{HSNO}$  (Figure 3A). The same experiment with  $\text{GS}^{15}\text{NO}$  additionally confirmed generation of  $\text{HS}^{15}\text{NO}$  (see Figure S4) in the reaction of  $\text{GS}^{15}\text{NO}$  and  $\text{H}_2\text{S}$  (Scheme 1, eq 3). No peaks of the putative  $[\text{HSSNO} + \text{H}]^+$  cation were detected, suggesting that this adduct is not present in solution.

The transnitrosation reaction was also characterized by FTIR spectroscopy. Difference FTIR spectra (Figure 3B) clearly show the disappearance of the  $\nu_{\text{NO}}$  vibration from GSNO at ~1515  $\text{cm}^{-1}$  with the appearance of a new signal of similar intensity at ~1568  $\text{cm}^{-1}$ . This frequency is slightly lower than that calculated for  $\text{HSNO}$  in the gas phase and measured in an argon matrix (1596  $\text{cm}^{-1}$  for the *trans*- and 1569  $\text{cm}^{-1}$  for the *cis*-isomer),<sup>10</sup> due to solvation effects.

When  $\text{GS}^{15}\text{NO}$  was used to prepare  $\text{HS}^{15}\text{NO}$ , the corresponding  $\text{N}=\text{O}$  vibration shifted to lower values (~1549  $\text{cm}^{-1}$  as compared to the calculated value of 1540  $\text{cm}^{-1}$  from the simple harmonic oscillator model) (inset to Figure 3B).

Finally,  $\text{HSNO}$  prepared in the reaction of  $^{15}\text{N}$ -enriched GSNO and  $\text{H}_2\text{S}$  was characterized by using  $^{15}\text{N}$  NMR spectroscopy. Addition of an equimolar amount of  $\text{Na}_2\text{S}$  led to the immediate disappearance of the GSNO peak (409 ppm) and appearance of a previously unidentified  $^{15}\text{N}$  resonance at 322 ppm (Figure 3C), which we assign to  $\text{HSNO}$ . This new chemical entity was stable for less than 1 h at pH 7.4 and 21 °C, with subsequent measurements showing only the nitrite signal at 247 ppm. A linear relationship exists between chemical shifts of *S*-nitrosothiols and the  $\text{pK}_a$  values of the corresponding thiols; a lower  $\text{pK}_a$  of a starting thiol implies smaller ppm values of  $^{15}\text{N}$  chemical shifts of the resulting *S*-nitrosothiol.<sup>14</sup> Therefore, the lower  $\text{pK}_a$  of  $\text{H}_2\text{S}$  in comparison to *R*-substituted thiols implies a smaller chemical shift of  $\text{HSNO}$  as compared to those of the substituted analogs. Furthermore, less electron density on S in the case of  $\text{HSNO}$  when compared to RSNO speaks in favor of a higher  $n \rightarrow \pi^*$  transition energy and a smaller  $^{15}\text{N}$  chemical shift.<sup>14</sup>

The yellow coloration of the solution, corresponding to the absorbance maximum at 412 nm (Figure S2), remains even after the  $^{15}\text{N}$  NMR peak and characteristic  $\text{N}=\text{O}$  vibration disappear from the solution spectra. This result, in agreement with our MS findings, excludes the presence of  $\text{SSNO}^-$ , which as a nitrogen atom-containing species would have displayed a

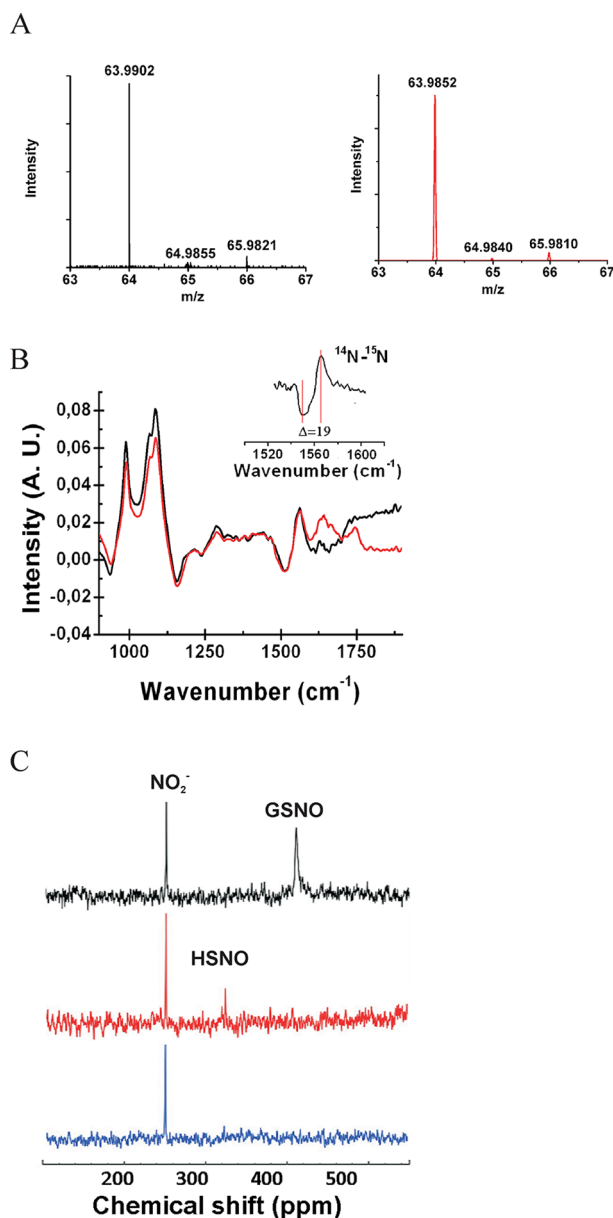


**Figure 3.** Characterization of HSNO/SNO<sup>−</sup> generated by transnitrosation of S-nitrosoglutathione (GSNO) and H<sub>2</sub>S. (A) ESI-TOF-MS spectrum of HSNO generated in transnitrosation reaction between GSNO and H<sub>2</sub>S. Experimental (black) and theoretical (red) isotope distribution of the detected *m/z* 64 peak of [HSNO + H]<sup>+</sup>. (B) Real-time FTIR confirms formation of a new nitrosothiol product. Differential IR spectrum of the reaction of 120 mM GSNO and 100 mM Na<sub>2</sub>S in 300 mM potassium phosphate buffer pH 7.4 (black, after 1 min; red, after 10 min). Inset: Spectral difference between <sup>14</sup>N and <sup>15</sup>N labeled HSNO/SNO<sup>−</sup>. (C) <sup>15</sup>N NMR spectrum of HSNO/SNO<sup>−</sup> at pH 7.4. Black: Mixture of <sup>15</sup>N-enriched GSNO with nitrite. Red: After addition of equimolar concentration (25 mM) of sulfide. Blue: After 1 h, only the nitrite signal remains. The reaction was performed in 300 mM potassium phosphate buffer, pH 7.4.

corresponding <sup>15</sup>N peak and N=O vibration band. Thus, the band at 412 nm results predominantly from the mixture of polysulfides.

Collectively, these experiments unambiguously confirm the presence of HSNO/SNO<sup>−</sup> in aqueous solution at pH 7.4 and demonstrate that it can be formed in a transnitrosation reaction between H<sub>2</sub>S and RSNOs (Scheme 1, eq 3).

### Chemical Biology of HSNO: Generation of NO<sup>•</sup>.

RSNOs may spontaneously decompose to give NO<sup>•</sup>, nitrosate a thiol, or form nitroxyl (HNO), as originally proposed.<sup>28</sup> Following the same reasoning (Scheme 1, eqs 4–6), we focused on characterizing the metabolic fate of HSNO.

Evidence for NO<sup>•</sup> production from HSNO was obtained by following the previously characterized transnitrosation reaction between GSNO and H<sub>2</sub>S, as a source of HSNO, in combination with simultaneous amperometric monitoring with the use of H<sub>2</sub>S- and NO<sup>•</sup>-sensitive electrodes. To minimize metal ion-catalyzed decomposition of S-nitrosothiols, buffers were thoroughly treated with Chelex 100 and supplemented with 100 μM neocuproine. Addition of GSNO to a buffered Na<sub>2</sub>S solution caused removal of free H<sub>2</sub>S with concomitant NO<sup>•</sup> formation (7 ± 3% based on total nitrogen) (Figure 4A). Similar results were obtained for the reaction of S-nitrosoalbumin and H<sub>2</sub>S (see Figure S5), confirming that the reaction also proceeds with high-molecular-weight RSNOs.

The release of NO<sup>•</sup> is a consequence of HSNO homolysis, as shown in eq 4 of Scheme 1. Taking into account the existence of the zwitterionic and ion-pair resonance structures (R–S<sup>+</sup>=N–O<sup>−</sup> and RS<sup>−</sup>/NO<sup>+</sup>, respectively), resulting in multireference character of the HSNO wave function, S–N bond length and dissociation energy for HSNO were computed to be 1.85 Å and 29.2 kcal/mol, respectively.<sup>8,9</sup> As compared to other S-nitrosothiols, HSNO should be slightly less stable and more prone to homolysis.<sup>8,9</sup> The kinetics of HSNO homolytic bond dissociation (eq 4, Scheme 1) can be determined on the basis of amperometric detection of NO release (Figure 4B).

For this first-order reaction, the corresponding rate constant was determined to be 0.12 ± 0.01 s<sup>−1</sup>. Conversely, the kinetics of the HSNO/SNO<sup>−</sup> formation reaction (eq 3 in Scheme 1), assuming that the side reactions<sup>29a</sup> and the spontaneous release of NO from GSNO<sup>29b</sup> are slower than the main transnitrosation reaction, were monitored following H<sub>2</sub>S consumption (Figure 4C) under second-order reaction conditions (GSNO:H<sub>2</sub>S ratio was 1:1, 250 μM each). The corresponding rate constant is 84 ± 7 M<sup>−1</sup> s<sup>−1</sup> at 25 °C. In comparison with other transnitrosation reactions (for S-nitroso-N-acetylpenicillamine (SNAP) + GSH, *k* = 9 M<sup>−1</sup> s<sup>−1</sup>; for SNAP + Cys, *k* = 21 M<sup>−1</sup> s<sup>−1</sup>),<sup>29c</sup> higher reactivity of H<sub>2</sub>S is expected.

### Chemical Biology of HSNO – Generation of HNO.

Recent studies showed that sulfide is produced in tissues at a high metabolic rate,<sup>30a</sup> the concentration in plasma being in the micromolar range<sup>30b</sup> and therefore in excess of what has been proposed to represent the physiological concentration range for RSNOs.<sup>6a,b</sup> Considering such concentrations, cellular HSNO/SNO<sup>−</sup> formation would be expected to yield nitroxyl (HNO/NO<sup>−</sup>) (Scheme 1, eq 5), the reduced form of NO<sup>•</sup> with distinct signaling properties.<sup>31a–c</sup> To prove its existence, reductive nitrosylation with methemoglobin was used.<sup>31d</sup> When a mixture of GSNO and H<sub>2</sub>S (1:2 molar ratios) was added to a buffered methemoglobin solution, immediate formation of nitrosyl-hemoglobin occurred (Figure 5A), whereas no spectral changes were observed with GSNO or H<sub>2</sub>S alone (see Figure S6). Nitroxyl also converts to nitrous oxide, N<sub>2</sub>O (*k* = 8 × 10<sup>6</sup> M<sup>−1</sup> s<sup>−1</sup>), reaction 13.<sup>31e</sup>



We therefore wanted to confirm the generation of nitroxyl along with that of NO<sup>•</sup> from HSNO using GC–MS (see Figure S7). Fifteen minutes after addition of an equimolar amount of H<sub>2</sub>S to GSNO, a moderate increase of the NO<sup>•</sup> amount was

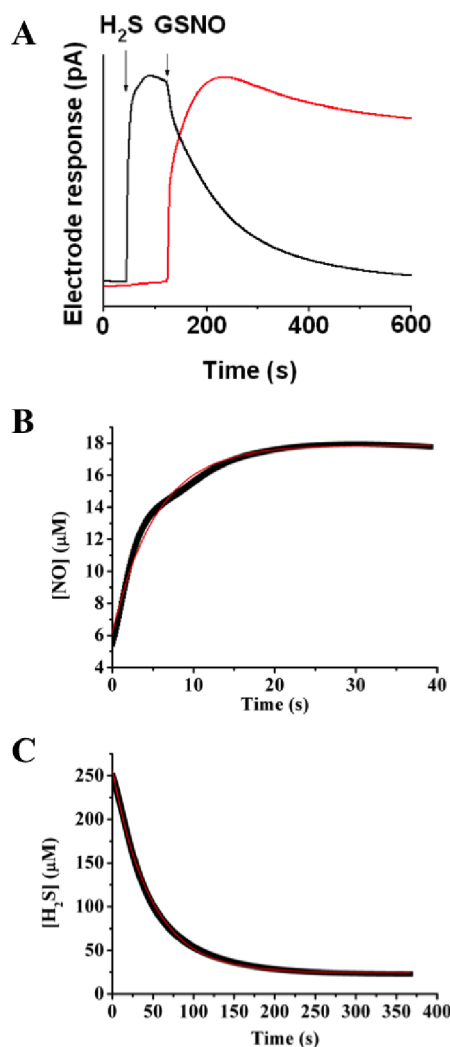
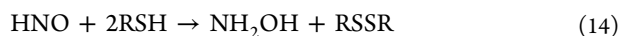


**Figure 4.** Kinetics of H<sub>2</sub>S consumption and NO generation in the reaction of GSNO with H<sub>2</sub>S. (A) Representative recordings by H<sub>2</sub>S (black) and NO• (red) electrodes, illustrating two processes described by eqs 3 and 4. A 400 μM Na<sub>2</sub>S solution was prepared in 50 mM potassium phosphate buffer, pH 7.4. When the electrode response reached its maximum, an equimolar amount of GSNO was added, triggering an immediate drop in current at the H<sub>2</sub>S electrode and a rise in the NO• signal. Kinetic traces of NO• release (B) and H<sub>2</sub>S consumption (C) from the reaction mixture containing 250 μM GSNO and 250 μM H<sub>2</sub>S at pH 7.4 at 25 °C. Red lines represent a first-order fit for (B) and a second-order fit for (C).

detected in the gas phase above the reaction mixture, in agreement with the NO• release detected by NO• electrode (Figure 2A). More importantly, an increased H<sub>2</sub>S concentration caused a large increase in the peak area of N<sub>2</sub>O (yield of 17 ± 5% calculated on the basis of total N content in starting GSNO solution) (see Figure S7).

HNO also reacts rapidly with thiols to give hydroxylamine, reaction 14.<sup>31a</sup>

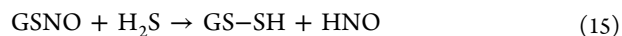


Assuming that excess H<sub>2</sub>S does react further with HNO generated in this manner, we wished to detect hydroxylamine. However, the use of standard colorimetric assays<sup>31f</sup> proved to be of no value for this purpose, because free thiols interfere with this assay, resulting in false negative results. For the present purpose, we therefore developed a rapid and

reproducible GC–MS method for detecting hydroxylamine based on its ability to react with ketones, cyclopentanone in the present case, to give corresponding oximes. Different reaction conditions corresponding to different ratios of GSNO and H<sub>2</sub>S were analyzed. Selected ion monitoring for the *m/z* 99 (cyclopentanone oxime) peak was applied. The maximal yield, observed for 10-fold excess of H<sub>2</sub>S over GSNO, was 71 ± 4% (Figure 5B). Together with the detected N<sub>2</sub>O and NO, this value corresponds to 112 ± 12% of total nitrogen consumed in the reaction. Some hydroxylamine (2 ± 1%) was detected when a 1:1 ratio was used, presumably due to the side reactions.

Although endogenous generation of HNO has never been detected directly in vivo, the recent development of a nitroxyl-responsive dye, CuBOT1,<sup>17</sup> enabled us to do so. When human umbilical vein endothelial cells, loaded with CuBOT1, were incubated with either GSNO or H<sub>2</sub>S (Figure S8), there was no change in fluorescence. Nitrogen monoxide releasing donor, diethylammonium (Z)-1-(N,N-diethylamino)diazen-1-ium-1,2-diolate (DEANONOate), also did not have any significant effect on CuBOT1 fluorescence, confirming the previous study of its selectivity.<sup>17</sup> Addition of both GSNO and H<sub>2</sub>S provided clear proof of HNO generation (Figure 5C,D). The effect was even more pronounced when cells were pretreated with GSNO to increase intracellular RSNO content, washed, and then loaded with the probe before exposure to H<sub>2</sub>S (Figure 5C,D).

These experiments strongly support the hypothesis that cellular HSNO is involved in the formation of nitroxyl, but they cannot exclude the possibility that HNO is produced directly in the reaction of GSNO and H<sub>2</sub>S (eq 15).



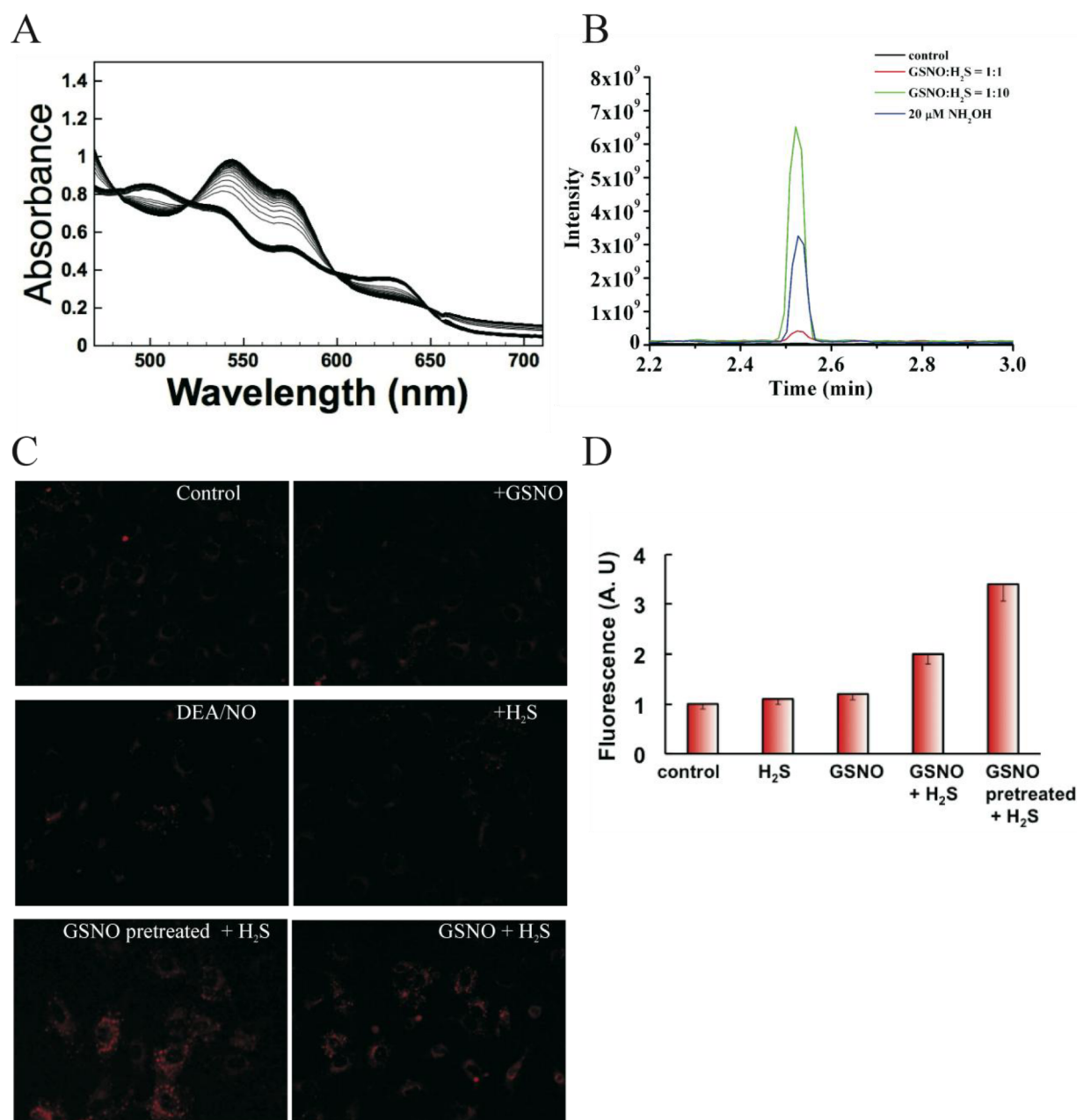
In particular, previous studies suggest that GSNO decomposes in the presence of GSH with the formation of GSSG,<sup>32</sup> which would imply the direct formation of HNO via eq 15. We found no evidence for such direct formation of HNO, for neither N<sub>2</sub>O nor NH<sub>2</sub>OH levels were significantly changed when GSNO was mixed with H<sub>2</sub>S in a 1:1 molar ratio (Figure 5B and Figure S7). Furthermore, no GSSH was detected in the ESI-TOF MS spectra (Figure S3). We further explored the possibility, however, by carrying out DFT calculations for the reaction of CH<sub>3</sub>SNO, as a model for S-nitrosothiols, with H<sub>2</sub>S/HS<sup>−</sup>.

Figure 6 (Table S1) shows the lowest-energy profile for the reaction of protonated (A) and deprotonated hydrogen sulfide (B). In both cases, the reaction can proceed by two pathways, H<sub>2</sub>S/HS<sup>−</sup> attack on either the N or the S atom of CH<sub>3</sub>SNO.

H<sub>2</sub>S attack on the N atom leads to the formation of CH<sub>3</sub>SH and HSNO molecules (**Final 1**) via transition state, **TS1**, with the activation barrier of 23.8 kcal mol<sup>−1</sup> (Figure 6A). The reaction via attack on the S atom of CH<sub>3</sub>SH is characterized by a much higher activation barrier (**TS2**, *E*<sub>act</sub> = 47.5 kcal mol<sup>−1</sup>) and leads to the formation of CH<sub>3</sub>S-SH and HNO (**Final 2**). Formation of CH<sub>3</sub>S-SH and HNO, **Final 2**, is also thermodynamically less favorable than formation of CH<sub>3</sub>SH and HSNO, **Final 1** (13.9 and 7.3 kcal mol<sup>−1</sup>, respectively, Figure 6A).

With HS<sup>−</sup>, the reaction proceeds in the same manner: the activation barrier for the N attack (**TS3**) is lower than that for the S attack (**TS4**) (5.8 vs 39.8 kcal mol<sup>−1</sup>, respectively), with favorable formation of the N attack products (**Final 3**, Figure 6B).





**Figure 5.** Generation of HNO from HSNO in biological milieu. (A) Reductive nitrosylation as a proof of HNO formation. 100  $\mu$ M GSNO and 200  $\mu$ M Na<sub>2</sub>S solution were added to 50  $\mu$ M metHb in 50 mM potassium phosphate buffer pH 7.4, and the reaction was followed every 10 s for a total of 5 min. Immediate formation of nitrosylhemoglobin is indicative of HNO. (B) GC–MS detection of hydroxylamine. A 60  $\mu$ M GSNO solution was mixed, at different ratios indicated in the figure, with H<sub>2</sub>S at pH 7.4, and after 10 min the reaction mixture was treated with cyclopentanone and methanol. At 1 h after the incubation, the corresponding mixtures were analyzed by GC–MS ( $m/z$  99 for cyclopentanone oxime). Buffer and a GSNO solution served as controls. (C) H<sub>2</sub>S and GSNO react in cells to yield HNO. Human umbilical vein endothelial cells, loaded with 10  $\mu$ M CuBOT1, were treated with either 100  $\mu$ M Na<sub>2</sub>S, 100  $\mu$ M GSNO, or both for 20 min. Some cells were pretreated with 100  $\mu$ M GSNO for 20 min to increase intracellular nitrosothiol content and then exposed to 100  $\mu$ M Na<sub>2</sub>S. A 100  $\mu$ M DEA/NONOate solution served as a negative control. (D) Fluorescence intensity was quantified using ImageJ, NIH ( $n = >30$  cells).

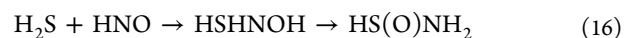
In addition, we estimate that HNO generation by eq 15 is energetically unfavorable by 40 kJ/mol by using standard electrode potentials and known bond energies (see the Supporting Information).

Whereas RSNO can exist as two isomers (*cis/trans*, with an energy difference of 0.8 kcal mol<sup>−1</sup>), regioselective attack on the N atom leads only to *cis*-HSNO, in agreement with the observed IR spectra.

Whether the same kinetics and thermodynamics operate for larger intracellular proteins remains to be determined. In the

light of recent suggestions that H<sub>2</sub>S acts through sulfhydrylation of protein thiol residues,<sup>3a,5b</sup> it is possible that direct reaction of RSNOs and H<sub>2</sub>S, with concomitant formation of HNO, takes place *in vivo*.

Sulfhydrylation of the proteins *in vivo* can be envisioned via another reaction mechanism. The reaction of hydroxylamine formation, given in eq 14, goes stepwise, and, for the case where H<sub>2</sub>S is reacting thiol, it would proceed as follows:





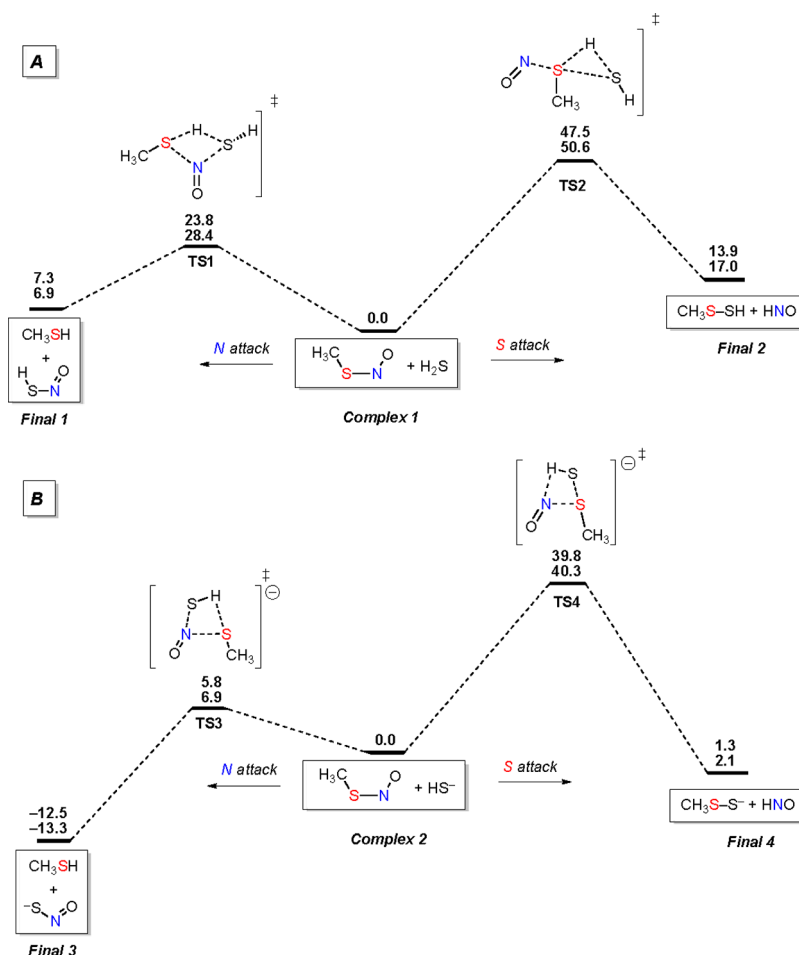


**Figure 6.** B3LYP/aug-cc-pVTZ computed energy profile for the reaction between  $\text{CH}_3\text{SNO}$  and  $\text{H}_2\text{S}/\text{HS}^-$ . Energies are in  $\text{kcal mol}^{-1}$ ;  $E+\text{ZPE}$  (first entry),  $G$  (second entry).



It is possible, however, that the product of the initial reaction,  $\text{HS(O)NH}_2$ , reacts further with protein thiols, particularly when  $\text{H}_2\text{S}$  is not present in large excess (eq 18), and form sulphydrylated protein with elimination of hydroxylamine.



**HSNO, a Diffusible Transnitrosating Agent.** Given its small size and reactive nature, HSNO might serve as a shuttle for nitrosonium equivalents by supporting sequential transnitrosation reactions. Equation 3 in Scheme 1 is slightly, ca. 10  $\text{kJ mol}^{-1}$ , uphill energetically, which is readily calculated<sup>33a</sup> from the minor difference (ca. 12  $\text{kJ}$  stronger) between bond strengths of  $\text{GS}-\text{NO}^{33b}$  and  $\text{HS}-\text{NO}$ ,<sup>8,9</sup> and the electrode potentials,  $E^\circ(\text{GS}^\bullet, \text{H}^+/\text{GSH}) = 0.94 \text{ V}^{33c}$  and  $E^\circ(\text{S}^\bullet, 2\text{H}^+/\text{H}_2\text{S}) = E^\circ(\text{S}^\bullet, \text{H}^+/\text{HS}^-) = 0.92 \text{ V}^{33d}$  at pH 7. Consequently, eq 6 in Scheme 1 is energetically favorable by the same amount.

To examine the feasibility of this scenario, we first investigated transnitrosation reactions between GSNO and bovine serum albumin (BSA) as a model. Albumin is proposed to be one of the carriers/storages of bioactive  $\text{NO}^\bullet$  in human plasma.<sup>34</sup> As a proof-of-concept experiment,  $\text{H}_2\text{S}$  was incubated with GSNO at 37 °C for 5 min to allow complete GSNO decomposition prior to the addition of albumin. After addition of BSA and a further 15 min incubation, the reaction mixture was analyzed by ESI-TOF MS. The peak shifts imply that four

nitroso equivalents per protein were added (see Figure S9). When the dialyzed HSNO-treated albumin sample was placed into buffer and irradiated with light, release of  $\text{NO}^\bullet$  was induced (see Figure S9), confirming S-nitrosation of BSA.

S-Nitrosoproteins are relatively stable and unless exposed to light or traces of heavy metals, they cannot exchange  $\text{NO}^+$  equivalents with other proteins through the membrane.<sup>6b</sup> Considering the potential significance of the shuttle function of HSNO, we designed an experiment specifically to address this notion (Figure 7A). Poly nitrosated albumin was placed inside a dialysis bag and inserted into a buffered solution of non-nitrosated albumin. In one of the samples,  $\text{H}_2\text{S}$  was injected into the dialysis bag containing BSA-SNO, while the untreated one served as a control. If HSNO were to be formed as a small neutral species, it should have been able to freely diffuse through the membrane and reach the outside solution of BSA. Without such intermediate, the exchange of  $\text{NO}^+$  equivalents between the compartments would be unlikely. After 5 min of incubation, the dialysis bags were removed and the exterior albumin solution was dialyzed for 2 h against water to remove traces of small molecules. Subsequent addition of aliquots of these solutions into  $\text{Cu}^{2+}$ -containing buffer (Figure 7B) revealed a clear  $\text{NO}^\bullet$  signal for  $\text{H}_2\text{S}$ -treated samples as detected by an  $\text{NO}^\bullet$  electrode, whereas control incubates showed only minor signals, most likely the result of metal contamination. RSNO quantification by the Saville assay showed that  $11 \pm 1\%$  of BSA became nitrosated in  $\text{H}_2\text{S}$ -treated samples as compared

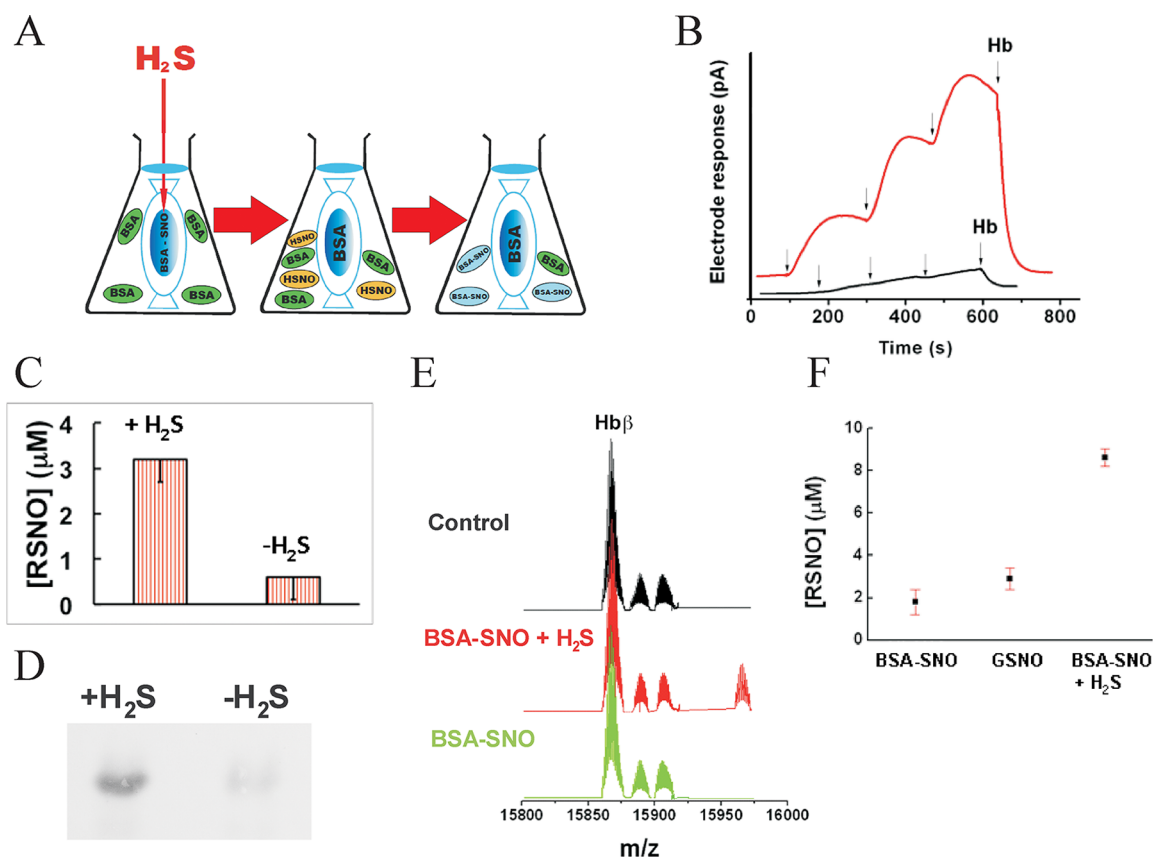


**Figure 7.** HSNO serves as a shuttle for NO<sup>+</sup>. (A) Experimental design for the protein-to-protein trans-nitrosation mediated by HSNO (see Experimental Section). (B) S-Nitrosothiol content in the sample obtained from protein-to-protein transnitrosation experiment. NO<sup>•</sup> electrode responses upon subsequent addition of aliquots of the control (black) or H<sub>2</sub>S-treated samples (red) into 500 μM ascorbate/Cu<sup>2+</sup> containing solution. Upon addition of hemoglobin (Hb), all NO<sup>•</sup> was scavenged. (C) Total amount of RSNOs generated by H<sub>2</sub>S in protein-to-protein transnitrosation experiment ( $n = 4$ ). (D) The results of the biotin switch assay for the same samples. (E,F) HSNO facilitated nitrosation of hemoglobin in human red blood cells. Deconvoluted mass spectra (E) of hemoglobin beta subunit isolated from RBC after the treatment with synthetic poly-S-nitrosoalbumin (BSA-SNO) in the presence or absence of H<sub>2</sub>S. Sample treated with poly-S-nitrosoalbumin in the presence of H<sub>2</sub>S exhibit another peak shifted by mass of 58 corresponding to [Hb - 2H + NO + K]<sup>+</sup>. S-Nitroso hemoglobin content (F) determined using Saville's method. Hemoglobin concentration in all samples was 650 μM.

to only  $2 \pm 1\%$  in the controls (Figure 7C), and these results were qualitatively confirmed with the biotin-switch assay (Figure 7D).

Additional experiments were carried out using human red blood cells (RBCs). S-Nitrosation of hemoglobin (Hb) is important for the regulation of oxygen delivery,<sup>35</sup> but the chemical basis for this process is still a matter of debate.<sup>6b,c</sup> To test whether HSNO could be a carrier from plasma S-nitrosoproteins to Hb, washed RBCs were incubated for 5 min in PBS supplemented with 30 μM poly-S-nitrosoalbumin (BSA-SNO),<sup>34a</sup> in the absence or presence of 50 μM Na<sub>2</sub>S. Hemoglobin was obtained after extensive washing of cells with PBS followed by hemolysis in nanopure water containing 100 μM neocuproine and analyzed by ESI-TOF-MS and Saville assay. Deconvoluted mass spectra (Figure 7E) revealed that the hemoglobin β-subunits (obtained mass  $15\,866.3 \pm 1$ , expected 15 867.2) of RBCs treated with nitrosoalbumin and Na<sub>2</sub>S exhibit an additional peak shifted by a mass of 58, indicative of the addition of 2NO moieties/Hb ([Hb - 2H + 2NO + K]<sup>+</sup>). For comparison, the total S-nitrosoprotein concentration was determined in the samples of Hb treated with GSNO, BSA-SNO, and BSA-SNO + H<sub>2</sub>S (Figure 7F).

There are several pathways by which GSNO or CysNO could traverse biological membranes and deliver the "NO<sup>+</sup>"

moiety. Some of them require a specific transporter or a thiol-to-thiol cascade transfer of "NO<sup>+</sup>".<sup>6b,c,37</sup> We wanted to test the observed superiority of HSNO over other low-molecular weight thiols to pass freely through membranes and S-nitrosate the targets faster. A 20 μL portion of washed packed RBC was diluted 100 times with PBS and exposed to 100 μM poly BSA-SNO in the presence or absence of 100 μM GSH, cysteine, or H<sub>2</sub>S for 2 min. After hemolysis, Hb was analyzed by LC-ESI-TOF-MS. Only in the case of H<sub>2</sub>S treatment was doubly S-nitrosated Hb β-subunit present in detectable quantities (Fig. S10). The alpha subunit remained unchanged. These data imply that, unlike GSNO and CysNO, HSNO can freely diffuse to reach its intracellular target and increase the intracellular HbSNO content.

**Physiological Significance.** Given the universal abundance of H<sub>2</sub>S and RSNOs in biological systems, it is plausible that HSNO is produced in vivo. The direct in vivo detection of HSNO, however, seemed challenging considering its demonstrated reactivity and relative instability. Nonetheless, we designed experiment to investigate its role in intracellular transnitrosation.<sup>36</sup>

If produced in cells, HSNO would be capable of further trans-nitrosation, so it is reasonable to assume that DAF-2 dye could serve as a sensor for its formation as well.

Mechanistically, the principle of this imaging technique involves a nitrosation step of DAF-2 to produce the fluorescence. We therefore tested the role of intracellularly produced  $\text{H}_2\text{S}$  on transnitrosation of DAF-2 induced by GSNO.

Cells were incubated in buffer supplemented with the inhibitor of  $\text{H}_2\text{S}$  producing enzyme (CSE), propargyl glycine (PG), washed and then exposed to GSNO. Whereas endothelial cell pretreatment with PG had no significant effects on basal DAF-2 fluorescence, it markedly blocked the GSNO-induced fluorescence increase (Figure 8A). CSE inhibition followed by sulfide treatment before exposure to GSNO restored GSNO-induced fluorescence, confirming that the effects were not due to unspecific quenching.

We demonstrate that endogenous  $\text{H}_2\text{S}$  is indeed involved in regulation of the intracellular S-nitrosation by an experiment in which HUVECs were exposed to the inhibitor of NO production (L- $\text{N}^{\text{G}}$ -nitroarginine methyl ester, L-NAME) or/and inhibitor of  $\text{H}_2\text{S}$  production (propargylglycine, PG).

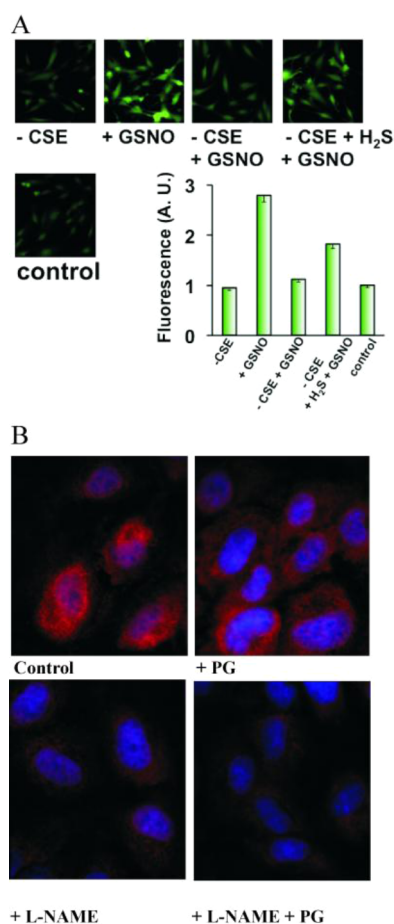


**Figure 8.** Endogenous  $\text{H}_2\text{S}$  controls transnitrosation and S-nitrosothiol formation. (A)  $\text{H}_2\text{S}$ -dependent GSNO-induced transnitrosation of DAF. HUVECs were incubated for 2 h in medium with or without CSE-inhibitor propargylglycine (1 mM). Cells were then exposed to 50  $\mu\text{M}$  GSNO. Some cells were additionally incubated with 100  $\mu\text{M}$   $\text{Na}_2\text{S}$  for 20 min prior to GSNO addition. NO-induced fluorescence was detected by fluorescence microscopy and quantified using ImageJ ( $n = 20$ –30 cells). (B) The effect of inhibitors of endogenous NO and  $\text{H}_2\text{S}$  production on intracellular S-nitrosation. HUVECs were exposed to medium supplemented without or with 1 mM L-NAME, 1 mM PG, or both for 2 h. Cells were fixed and intracellular RSNOs visualized by immunocytochemistry using anti-S-nitrosocysteine antibodies.

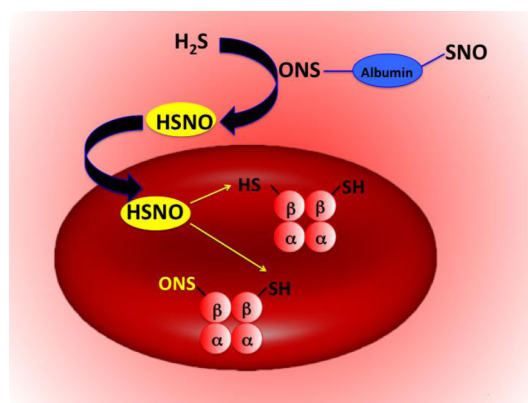


**Figure 9.** Proposed reaction scheme for HSNO-induced nitrosation of hemoglobin.

Exposure to PG lowered the level of intracellular SNOs as detected using specific S-nitrosocysteine antibodies (Figure 8B). L-NAME had a much stronger effect, as expected, but did not completely block S-nitrosation because it is a competitive inhibitor of nitric oxide synthase. An inhibitory effect was, however, most obvious when cells were exposed to both L-NAME and PG (Figure 8B). These results suggest an important role of intracellular  $\text{H}_2\text{S}$  in transnitrosation reactions.

The unique physicochemical properties of HSNO make it an excellent candidate for redox sensing and regulation of metabolic activities. In particular, HSNO could lead to the generation of HNO, which has significant cardio-pharmacological potential, and herein we provide the first direct intracellular detection of its generation. HNO has been also suggested to be involved in  $\text{H}_2\text{S}$  induced cardioprotection.<sup>4b</sup> Additionally, HSNO/SNO<sup>−</sup> might serve to facilitate further trans-nitrosation/denitrosation of other targets in the cell or even intercellularly, due to the facile diffusion ability of HSNO (as the neutral form of the HSNO/SNO<sup>−</sup> acid–base couple). Hemoglobin is one possible target, and the chemical mechanism of its S-nitrosation is still a matter of debate. S-Nitrosothiols (RSNOs) cannot cross cell membranes by free diffusion,<sup>6b,37</sup> and “NO<sup>+</sup>” transport has long been proposed to be facilitated by formation of smaller S-nitrosothiols, especially those of cysteine and/or glutathione, which may require specific transporters.<sup>37</sup> Formation of HSNO/SNO<sup>−</sup> might link plasma S-nitrosothiols to intracellular S-nitrosohemoglobin. Circulating  $\text{H}_2\text{S}$  could react with RSNOs forming HSNO/SNO<sup>−</sup> by transnitrosation, where HSNO would then freely diffuse across the RBC membrane to transfer its “NO<sup>+</sup>” moiety to the  $\beta$ -subunit of hemoglobin forming S-nitrosohemoglobin (Figure 9), known to have important physiological functions.<sup>35</sup>

Three key proteins presently accepted as major targets for  $\text{H}_2\text{S}$  and its subsequent regulation of blood pressure,<sup>2</sup> neuronal activity,<sup>38a</sup> and cardioprotection,<sup>38b</sup> the  $\text{K}_{\text{ATP}}$  channel, NMDA receptor, and NRF-2, respectively, are shown to be regulated by S-nitrosation.<sup>39</sup> Early<sup>5a</sup> and recent<sup>4d</sup> work suggests that activity of NO<sup>•</sup> synthase is a prerequisite for  $\text{H}_2\text{S}$  to exhibit its effect. The present study thus offers a chemical perspective into the metabolic fate of  $\text{H}_2\text{S}$  and opens a new chapter in biological chemistry of redox signaling.



## ■ ASSOCIATED CONTENT

## ■ Supporting Information

Supporting text, supporting table, and supporting Figures S1–S10. This material is available free of charge via the Internet at <http://pubs.acs.org>.

## ■ AUTHOR INFORMATION

## Corresponding Author

milos.filipovic@chemie.uni-erlangen.de

## Notes

The authors declare no competing financial interest.

## ■ ACKNOWLEDGMENTS

We thank Dr. Leeane Nye (University of Erlangen-Nürnberg) for technical help with ESI-TOF MS measurements and Dr. Achim Zahl (University of Erlangen-Nürnberg) for help with  $^{15}\text{N}$  NMR measurements. This work was supported by the intramural grant from University Erlangen-Nürnberg (Emerging Field Initiative: Medicinal Redox Inorganic Chemistry). T.N. and W.H.K. acknowledge the support from ETH Zürich. Work in the lab of S.J.L. was supported by a grant from the National Science Foundation. M.R. acknowledges the NIH for a postdoctoral fellowship.

## ■ REFERENCES

- (1) (a) Koppenol, W. H. *Free Radical Biol. Med.* **1998**, *25*, 385–391. (b) Ford, P. C.; Lorkovic, I. *Chem. Rev.* **2002**, *102*, 993–1018. (c) McCleverty, J. A. *Chem. Rev.* **2002**, *102*, 403–418. (d) Tennyson, A. G.; Lippard, S. J. *Chem. Biol.* **2011**, *18*, 1211–1220. (e) Stamler, J. S.; Singel, D. J.; Loscalzo, J. *Science* **1992**, *258*, 1898–1902. (f) Moncada, S.; Palmer, R. M. J.; Higgs, E. A. *Pharmacol. Rev.* **1991**, *43*, 109–142. (g) Calabrese, V.; Cornelius, C.; Rizzarelli, E.; Owen, J. B.; Dinkova-Kostova, A. T.; Butterfield, D. A. *Antioxid. Redox Signaling* **2009**, *11*, 2717–2739. (h) Palmer, R. M. J.; Ferrige, A. G.; Moncada, S. *Nature* **1987**, *327*, 524–526.
- (2) Yang, G.; Wu, L.; Jiang, B.; Yang, W.; Qi, J.; Cao, K.; Meng, Q.; Mustafa, A. K.; Mu, W.; Zhang, S.; Snyder, S. H.; Wang, R. *Science* **2008**, *322*, 587–590.
- (3) (a) Li, L.; Rose, P.; Moore, P. K. *Annu. Rev. Pharmacol. Toxicol.* **2011**, *51*, 169–187. (b) Kabil, O.; Banerjee, R. J. *Biol. Chem.* **2010**, *285*, 21903–21907. (c) Li, L.; Hsu, A.; Moore, P. K. *Pharmacol. Ther.* **2009**, *123*, 386–400.
- (4) (a) Whiteman, M.; Li, L.; Kostetski, I.; Chu, S. H.; Siau, J. L.; Bhatia, M.; Moore, P. K. *Biochem. Biophys. Res. Commun.* **2006**, *343*, 303–310. (b) Yong, Q. C.; Hu, L. F.; Wang, S.; Huang, D.; Bian, J. S. *Cardiovasc. Res.* **2010**, *88*, 482–491. (c) Ondrias, K.; Stasko, A.; Cacanyiova, S.; Sulova, Z.; Krizanov, O.; Kristek, F.; Malekova, L.; Knezl, V.; Breier, A. *Pfluegers Arch.* **2008**, *457*, 271–279. (d) Sojitra, B.; Bulani, Y.; Putcha, U. K.; Kanwal, A.; Gupta, P.; Kuncha, M.; Banerjee, S. K. *Mol. Cell. Biochem.* **2012**, *360*, 61–69. (e) Bertova, A.; Cacanyiova, S.; Kristek, F.; Krizanov, O.; Ondrias, K.; Tomaskova, Z. *Gen. Physiol. Biophys.* **2010**, *29*, 402–410.
- (5) (a) Zhao, W.; Wang, R. *Am. J. Physiol.: Heart Circ. Physiol.* **2002**, *283*, H474–H480. (b) Mustafa, A. K.; Sikka, G.; Gazi, S. K.; Steppan, J.; Jung, S. M.; Bhunia, A. K.; Barodka, V. M.; Gazi, F. K.; Barrow, R. K.; Wang, R.; Amzel, L. M.; Berkowitz, D. E.; Snyder, S. H. *Circ. Res.* **2011**, *109*, 1259–1268.
- (6) (a) Foster, M. W.; Hees, D. T.; Stamler, J. S. *Trends Mol. Med.* **2009**, *15*, 391–404. (b) Hogg, N. *Annu. Rev. Pharmacol. Toxicol.* **2002**, *42*, 585–600. (c) Keszler, A.; Zhang, Y.; Hogg, N. *Free Radical Biol. Med.* **2010**, *48*, 55–64. (d) Lima, B.; Forrester, M. T.; Hess, D. T.; Stamler, J. S. *Circ. Res.* **2010**, *106*, 633–646. (e) Hess, D. T.; Stamler, J. S. *J. Biol. Chem.* **2012**, *287*, 4411–4418. (f) Nakamura, T.; Lipton, S. A. *Antioxid. Redox Signaling* **2011**, *14*, 1479–1492. (g) Tegeder, I.; Scheving, R.; Wittig, I.; Geisslinger, G. *Pharmacol. Rev.* **2011**, *63*, 366–389. (h) Stamler, J. S.; Hess, D. T. *Nat. Cell Biol.* **2010**, *12*, 1024–1026. (i) Benhar, M.; Forrester, M. T.; Hess, D. T.; Stamler, J. S. *Science* **2008**, *320*, 1050–1054.
- (7) IUPAC nomenclature of the chemical compounds: HSNO, nitrososulfane or (hydrosulfanido)oxidonitrogen;  $\text{NO}^\bullet$ , oxidonitrogen( $\bullet$ );  $\text{HNO}_2$ , hydroxidooxidonitrogen;  $\text{H}_2\text{S}$ , dihydrosulfur;  $\text{HNO}$ , hydrido-oxidonitrogen;  $\text{NO}^-$ , oxidonitrate(1–);  $\text{NO}^+$ , oxidonitrogen(+);  $\text{N}_2\text{O}$ , oxidodinitrogen.
- (8) Timerghazin, Q. K.; English, A. M.; Peslherbe, G. H. *Chem. Phys. Lett.* **2008**, *454*, 24–29.
- (9) Timerghazin, Q. K.; Peslherbe, G. H.; English, A. M. *Phys. Chem. Chem. Phys.* **2008**, *10*, 1532–1539.
- (10) (a) Nonella, M.; Huber, J. R.; Ha, T.-K. *J. Phys. Chem.* **1987**, *91*, 5203–5209. (b) Structural isomer of HSNO is known as thionylimide (HNSO). Kirchhoff, W. H. *J. Am. Chem. Soc.* **1969**, *91*, 20437–20442.
- (11) Seel, F.; Kuhn, R.; Simon, G.; Wagner, M.; Krebs, B.; Dartmann, M. Z. *Naturforsch., B* **1985**, *40b*, 1607–1617.
- (12) Hughes, M. N.; Centelles, M. N.; Moore, K. P. *Free Radical Biol. Med.* **2009**, *47*, 1346–1353.
- (13) Filipovic, M. R.; Miljkovic, J.; Algaeuer, A.; Chario, R.; Shubina, T.; Herrmann, M.; Ivanovic-Burmazovic, I. *Biochem. J.* **2012**, *441*, 609–621.
- (14) Wang, K.; Hou, Y.; Zhang, W.; Ksebeti, M. B.; Xian, M.; Cheng, J.-P.; Wang, P. G. *Bioorg. Med. Chem. Lett.* **1999**, *9*, 2897–2902.
- (15) Karmann, W.; Meissner, G.; Henglein, A. Z. *Naturforsch., B* **1967**, *22*, 273–282.
- (16) Nauser, T.; Dockheer, S.; Kissner, R.; Koppenol, W. H. *Biochemistry* **2006**, *45*, 6038–6043.
- (17) Rosenthal, J.; Lippard, S. J. *Am. Chem. Soc.* **2010**, *132*, 5536–5537.
- (18) Gorren, A. C.; Schrammel, A.; Schmidt, K.; Mayer, B. *Arch. Biochem. Biophys.* **1996**, *330*, 219–228.
- (19) Stamler, J. S.; Feelisch, M. Preparation and Detection of S-Nitrosothiols. In *Methods in Nitric Oxide Research*; Feelisch, M., Stamler, J. S., Eds.; John Wiley & Sons: Chichester, England, 1996; pp 521–539.
- (20) Wang, X.; Kettenhofen, N. J.; Shiva, S.; Hogg, N.; Gladwin, M. T. *Free Radical Biol. Med.* **2008**, *44*, 1362–1372.
- (21) Mamone, G.; Sannolo, N.; Malorni, A.; Ferranti, P. *FEBS Lett.* **1999**, *462*, 241–245.
- (22) (a) Becke, A. D. In *The Challenge of d- and f-electrons: Theory and Computation*; Salahub, D. R.; Zerner, M. C., Eds.; American Chemical Society: Washington, DC, 1989; Chapter 12, p 165. (b) Vosko, S. H.; Wilk, L.; Nusair, M. *Can. J. Phys.* **1980**, *58*, 1200. (c) Lee, C.; Yang, W.; Parr, R. G. *Phys. Rev. B* **1988**, *37*, 785. (d) Becke, A. D. *J. Chem. Phys.* **1993**, *98*, 5648. (e) Kendall, R. A.; Dunning, T. H., Jr.; Harrison, R. J. *J. Chem. Phys.* **1992**, *96*, 6796–6806. (f) Woon, D. E.; Dunning, T. H., Jr. *J. Chem. Phys.* **1993**, *98*, 1358–13571. (g) Dunning, T. H., Jr. *J. Chem. Phys.* **1989**, *90*, 1007–1023.
- (23) Frisch, M. J.; Trucks, G. W.; Schlegel, H. B.; Scuseria, G. E.; Robb, M. A.; Cheeseman, J. R.; Scalmani, G.; Barone, V.; Mennucci, B.; Petersson, G. A.; Nakatsuji, H.; Caricato, M.; Li, X.; Hratchian, H. P.; Izmaylov, A. F.; Bloino, J.; Zheng, G.; Sonnenberg, J. L.; Hada, M.; Ehara, M.; Toyota, K.; Fukuda, R.; Hasegawa, J.; Ishida, M.; Nakajima, T.; Honda, Y.; Kitao, O.; Nakai, H.; Vreven, T.; Montgomery, J. A., Jr.; Peralta, J. E.; Ogliaro, F.; Bearpark, M.; Heyd, J. J.; Brothers, E.; Kudin, K. N.; Staroverov, V. N.; Kobayashi, R.; Normand, J.; Raghavachari, K.; Rendell, A.; Burant, J. C.; Iyengar, S. S.; Tomasi, J.; Cossi, M.; Rega, N.; Millam, J. M.; Klene, M.; Knox, J. E.; Cross, J. B.; Bakken, V.; Adamo, C.; Jaramillo, J.; Gomperts, R.; Stratmann, R. E.; Yazyev, O.; Austin, A. J.; Cammi, R.; Pomelli, C.; Ochterski, J. W.; Martin, R. L.; Morokuma, K.; Zakrzewski, V. G.; Voith, G. A.; Salvador, P.; Dannenberg, J. J.; Dapprich, S.; Daniels, A. D.; Farkas, Ö.; Foresman, J. B.; Ortiz, J. V.; Cioslowski, J.; Fox, D. J. *Gaussian 09*, revision B.1; Gaussian, Inc.: Wallingford, CT, 2009.
- (24) (a) Mills, G.; Schmidt, K. H.; Matheson, M. S.; Meisel, D. J. *Phys. Chem.* **1987**, *91*, 1590–96. (b) Chivers, T.; Da Silva, A. B. F.; Treu, O., Jr.; Trsic, M. *J. Mol. Struct.* **1987**, *162*, 351–357.



- (25) Quiroga, S. L.; Almaraz, A. E.; Amorebieta, V. T.; Perissinotti, L. L.; Olabe, J. A. *Chem.-Eur. J.* **2011**, *17*, 4145–4156.
- (26) Seel, F.; Wagner, M. Z. *Anorg. Allg. Chem.* **1988**, *558*, 189–192.
- (27) Munro, A. P.; Williams, L. H. *J. Chem. Soc., Perkin Trans. 2* **2000**, 1794–1797.
- (28) Arnelle, D. R.; Stamler, J. S. *Arch. Biochem. Biophys.* **1995**, *318*, 279–285.
- (29) (a) Sonnenschein, K.; de Groot, H.; Kirsch, M. *J. Biol. Chem.* **2004**, *279*, 45433–45440. (b) Meyer, D. J.; Kramer, H.; Özer, N.; Coles, B.; Ketterer, B. *FEBS Lett.* **1994**, *345*, 177–180. (c) Singh, R. J.; Hogg, N.; Joseph, J.; Kalyanaraman, B. *J. Biol. Chem.* **1996**, *271*, 28596–18603.
- (30) (a) Vitvitsky, V.; Kabil, O.; Banerjee, R. *Antioxid. Redox Signaling* **2012**, *17*, 22–31. (b) Shen, X.; Pattillo, C. B.; Pardue, S.; Bir, S. C.; Wang, R.; Kevil, C. G. *Free Radical Biol. Med.* **2011**, *50*, 1021–1031.
- (31) (a) Flores-Santana, W.; Salmon, D. J.; Donzelli, S.; Switzer, C. H.; Basudhar, D.; Ridnour, L.; Cheng, R.; Glynn, S. A.; Paolocci, N.; Fukuto, J. M.; Miranda, K. M.; Wink, D. A. *Antioxid. Redox Signaling* **2011**, *14*, 1659–1674. (b) Fukuto, J. M.; Carrington, S. J. *Antioxid. Redox Signaling* **2011**, *14*, 1649–1658. (c) Fukuto, J. M.; Switzer, C. H.; Miranda, K. M.; Wink, D. A. *Annu. Rev. Pharmacol. Toxicol.* **2005**, *45*, 335. (d) Bazylinski, D. A.; Hollocher, T. C. *J. Am. Chem. Soc.* **1985**, *107*, 7982–7986. (e) Miranda, K. M.; Dutton, A. S.; Ridnour, L. A.; Foreman, C. A.; Ford, E.; Paolocci, N.; Katori, T.; Tocchetti, C. G.; Mancardi, D.; Thomas, D. D.; Espey, M. G.; Houk, K. N.; Fukuto, J. M.; Wink, D. A. *J. Am. Chem. Soc.* **2005**, *127*, 722–731. (f) Wink, D. A.; Feelisch, M. Formation and detection of nitroxyl and nitrous oxide. In *Methods in Nitric Oxide Research*; Feelisch, M., Stamler, J. S., Eds.; John Wiley & Sons: Chichester, England, 1996; pp 403–412.
- (32) Singh, S. P.; Wishnok, J. S.; Keshive, M.; Deen, W. M.; Tannenbaum, S. R. *Proc. Natl. Acad. Sci. U.S.A.* **1996**, *93*, 14428–14433.
- (33) (a) Koppenol, W. *Inorg. Chem.* **2012**, *51*, 5637–5641. (b) Bartberger, M. D.; Mannion, J. D.; Powell, S. C.; Stamler, J. S.; Houk, K. N.; Toone, E. J. *J. Am. Chem. Soc.* **2001**, *123*, 8868–8869. (c) Folkes, L. K.; Trujillo, M.; Bartesaghi, S.; Radi, R.; Wardman, P. *Arch. Biochem. Biophys.* **2011**, *506*, 242–249. (d) Das, T. N.; Huie, R. E.; Neta, P.; Padmaja, S. *J. Phys. Chem. A* **1999**, *103*, 5221–5226.
- (34) (a) Simon, D. I.; Mullins, M. E.; Jia, L.; Gaston, B.; Singel, D. J.; Stamler, J. S. *Proc. Natl. Acad. Sci. U.S.A.* **1996**, *93*, 4763–4741. (b) Orie, N. N.; Vallance, P.; Jones, D. P.; Moore, K. P. *Am. J. Physiol.: Heart Circ. Physiol.* **2005**, *289*, H916–H923.
- (35) (a) Singel, D. J.; Stamler, J. S. *Annu. Rev. Physiol.* **2005**, *67*, 99. (b) Jia, L.; Bonaventura, C.; Bonaventura, J.; Stamler, J. S. *Nature* **1996**, *380*, 221–226. (c) Reynolds, J. D.; Hess, D. T.; Stamler, J. S. *Transfusion* **2011**, *51*, 852–858.
- (36) Planchet, E.; Keiser, W. E. *J. Exp. Bot.* **2006**, *57*, 3043–3055.
- (37) (a) Zhang, Y.; Hogg, N. *Proc. Natl. Acad. Sci. U.S.A.* **2004**, *101*, 7891–7896. (b) Bronlowska, K. A.; Zhang, Y.; Hogg, N. *J. Biol. Chem.* **2006**, *281*, 33835–33841.
- (38) (a) Gadalla, M. M.; Snyder, S. H. *J. Neurochem.* **2010**, *113*, 14–26. (b) Calvert, J. W.; Jha, S.; Gundewar, S.; Elrod, J. W.; Ramachandran, A.; Pattillo, C. B.; Kevil, C. G.; Lefer, D. J. *Circ. Res.* **2009**, *105*, 365–374.
- (39) (a) Kawano, T.; Zoga, V.; Kimura, M.; Liang, M. Y.; Wu, H. E.; Gemes, G.; McCallum, J. B.; Kwok, W. M.; Hogan, Q. H.; Sarantopoulos, C. D. *Mol. Pain* **2009**, *5*, 12. (b) Lipton, S. A.; Choi, Y. B.; Takahashi, H.; Zhang, D.; Li, W.; Godzik, A.; Bankston, L. A. *Trends Neurosci.* **2002**, *25*, 474–480. (c) Um, H. C.; Jang, J. H.; Kim, D. H.; Lee, C.; Surh, Y. J. *Nitric Oxide* **2011**, *25*, 161–168.